Composite Structures, 183 (1) 510-520 (2018)
http://dx.doi.org/10.1016/j.compstruct.2017.05.059

MATRIX CRACKING EVOLUTION IN OPEN-HOLE LAMINATES SUBJECTED TO THERMO-MECHANICAL LOADS

M. M. Moure[a], S. K. García-Castillo[a], S. Sánchez-Sáez[a], E. Barbero[a*], E. J. Barbero[b]

[a] Department of Continuum Mechanics and Structural Analysis, University Carlos III of Madrid, Avda de la Universidad 30, 28911 Leganés, Madrid, Spain

[b] Mechanical and Aerospace Engineering, West Virginia University, Morgantown, WV 26506, USA

Abstract

In this work, a constitutive model is developed and used to predict matrix cracking and fiber damage evolution in all the plies of symmetric laminates when both mechanic and thermal loads are applied. A model previously developed is modified to take into account the thermal stresses that appear in each ply when the temperature is reduced below the Stress Free Temperature. Data of matrix damage initiation and evolution due to thermomechanical loads for four materials and six laminate lay-ups taken from the scientific literature are used to validate the model. A good correlation between the predictions and the experimental results is found. The model is used to analyze the thermomechanical damage in laminates containing a centered hole subjected to in-plane tensile loads. It is observed that the thermal load alone does not produce a stress concentration around the hole but the thermal residual stress accelerates damage accumulation during mechanical load.

Keywords: Open-hole laminates; Thermomechanical; Transverse cracking; Finite element analysis; Discrete damage mechanics

1. INTRODUCTION

Composite laminates are widely used in aerospace and aircraft industries, in structural applications such as pressure vessels, aircraft fuselage, etc. These structures are subjected to in-plane loads [1] and temperatures between -250º and 120ºC [2]. Sometimes, these components contain thousands of holes for joining purpose or cut-outs for opening accesses. The presence of a hole on a laminate produces a stress gradient that increases the stress field in its proximity. This phenomenon changes the failure mechanisms of the laminate and produces a reduction of the failure strength of the structure compared to that with no hole.

Composite Structures, 183 (1) 510-520 (2018)
http://dx.doi.org/10.1016/j.compstruct.2017.05.059

When a composite laminate subjected to thermal and/or mechanical loading is stressed, several damage mechanisms such as matrix microcracking, delamination, and fiber breakage are observed before final failure [3]. Matrix cracking is usually the first failure mechanism in appear, and occurs at load levels below the failure load of the laminate [4, 5]. When a thermal load is applied to the laminate, cracks appear mainly due to the mismatch in the Poisson´s ratio and/or coefficient of thermal expansion between adjacent plies of different orientation. Usually, this damage mode does not lead to overall failure of the composite laminate. However, matrix cracking is an important failure mechanism because it induces other damage modes, degrades the mechanical properties, and increases the permeability of the laminate to gases and liquids [3-7]. Matrix cracking can also occur in some laminates only due to thermal effects. As the temperature decreases from the stress-free temperature, residual stresses appear in the material. When these stresses become large enough, matrix cracking and delamination may appear [8-9]. Depending on the laminate stacking sequence, ply clustering, and the presence or absence of free edges, either matrix cracking of delamination may be predominant. This study focuses on laminates where matrix cracking and fiber breakage are predominant and delamination is negligible.

Many authors have studied the degradation of the mechanical properties in laminates due to evolution of the matrix cracking [5, 6, 10--13], fiber damage [6,23,39], which may be studied by models based on Continuum Damage Mechanics (CDM) [5, 10, 11, 39], Crack Opening Displacement (COD) models [14-22], Discrete Damage Mechanics (DDM) [6, 12, 13] and so on. The DDM [12] model has been evaluated for open-hole laminates subjected to mechanical loads [6,23] but the effect of thermal loads and thermal residual stresses have not been studied.

In general, the problem of intralaminar cracking in composite laminates subjected to mechanical in-plane loads (static and fatigue) is extensively studied [6, 12, 15-25], but only a few studies are focused on laminates subjected to thermal loads. Few works about the behavior of an open-hole laminate subjected to thermal or thermo-mechanical loads are available in the scientific literature [7, 26-30]. Therefore, more work is needed to understand the behavior of laminates subjected to thermomechanical loads, especially in those cases where stress gradients are present, as those caused by open holes. Particularly useful is the development of numerical models to predict the cracking evolution in laminates subjected to thermomechanical loads, which can be used as design tools for composite structures.

In this work, the evolution of the matrix cracking in open-hole composite laminates subjected to thermomechanical loads is studied. For that purpose, the DDM model of Barbero-Cortes is modified to

incorporate the effect of thermal loads. The modified model is then validated for different materials and laminates under thermal-only, mechanical-only, and combined thermo-mechanical loads. The effect of thermal load (without mechanical load) and mechanical load in the stress concentration and damage evolution in open-hole laminates are analyzed.

2. NUMERICAL MODEL DESCRIPTION

The Discrete Damage Mechanic (DDM) model used in this work was originally developed by Barbero and Cortes in 2010 [12]. This model is able to predict the matrix cracking evolution in all the plies of symmetric laminates subjected to in-plane loads. In a previous work, the fiber failure damage mechanism was added in order to predict the final failure of the laminate [6,31]. An in depth description of the model can be found in [12] and [6]. This model has been previously validated with experimental results in terms of matrix cracking evolution and failure strength without thermal load or residual stresses [6]. In this work, a new modification is introduced in the model to perform thermomechanical analysis. There are two issues to deal with this new modification: laminate thermal strain and computation of energy release rate.

2.1. Laminate thermal strain

When embedded in finite element analysis software such as Abaqus, DDM model calculates the force vector N as

$$N = [A]\{\epsilon + \Delta\epsilon\} \quad \text{(Eq.1)}$$

where ϵ is the strain from the last converged step, $\Delta\epsilon$ is the increment of strain that the Newton-Raphson algorithm attempts for the current step and $[A]$ is the plain stiffness matrix. To include thermal effects, thermal stress is added to the force vector as follows

$$N = [A]\{\epsilon + \Delta\epsilon - \alpha^{\circ}\delta T\} \quad \text{(Eq.2)}$$

where α° is the Coefficient of Thermal Expansion (CTE) of the damaged laminate, and δT is the temperature variation, and is defined as

$$\delta T = T + \Delta T - SFT \quad \text{(Eq.3)}$$

being T the temperature of the last converged step, ΔT the increment of temperature that the Newton-Raphson algorithm attempts for the current step, and SFT is the Stress Free Temperature of the material, which is usually taken to be equal to the curing temperature or the glass transition temperature of the polymer.

Note that δT is always measured with respect to the stress-free temperature of the material. Therefore, to avoid convergence problems, it is best to set the initial temperature of the whole model to SFT. It is well know that residual stress has to be calculated from the SFT because that is the only temperature where the stress can be assumed to be zero [32-35].

The laminate CTE $\{\alpha^0\}$, is calculated as follows [6.56, 36]. Fist, the thermal stress $\{N^T\}$ is calculated

$$\{N^T\} = \sum_{k=1}^{N} [\bar{Q}]\{\bar{\alpha}\}t_k \qquad \text{(Eq.4)}$$

where overbar means the quantity has been transformed to laminate coordinate system (c.s.); $[\bar{Q}]$ is the damaged stiffness of the lamina *k* in laminate c.s; $\bar{\alpha}$ is the intact CTE of the lamina *k* in laminate c.s; and t_k is the thickness of lamina *k*. The CTE is defined as the strain corresponding to $\Delta T = 1$ and thus coordinate transformation of CTE is performed as a strain (Eq.5.44 of [36]), i.e.,

$$\bar{\alpha}^k = [R][T^{-1}][R^{-1}]\alpha^k \qquad \text{(Eq.5)}$$

where $[R]$ is the Reuter matrix, $[T^{-1}]$ is the inverse of the transformation matrix and α^k is the intact CTE of lamina *k* in lamina c.s.

Finally, the laminate CTE is computed as [6.62, 36]

$$\{\alpha^0\} = [A]^{-1}\{N^T\} \qquad \text{(Eq.6)}$$

2.2. Energy release rate

The energy release rate G is computed as

$$G = \frac{U_a - U_b}{\Delta A} \qquad \text{(Eq.7)}$$

where U_a and U_b are the elastic strain energies of the representative volume element (RVE, Fig. 1) for crack densities λ_a and $\lambda_b = 2\lambda_a$; and $\Delta A = l_1 \cdot t_c$ is the increment of crack area when a new crack propagates in a lamina with thickness t_c. Note that the dimension of the RVE is $l_1 = 1.0$ along the fiber direction of the cracking lamina ($k = c$) and that a new crack propagates unstably (section 7.2.1 of [36]) through the thickness t_c and parallel to the fiber direction in lamina *c*.

The elastic strain energy U must be calculated by adding the individual contributions of each lamina

$$U = \frac{1}{2H}\sum_{k=1}^{n} t_k\left(\epsilon - \alpha^{(k)}\delta T\right) \cdot \; Q^{(k)} \cdot \; \left(\epsilon - \alpha^{(k)}\delta T\right) \qquad \text{(Eq.8)}$$

where $H = \sum_{k=1}^{n} t_k$ is the laminate thickness, *n* is the number of laminas in the laminate, and all the quantities in (Eq.8) are expressed in the c.s. of the cracking lamina (k=c).

Composite Structures, 183 (1) 510-520 (2018)
http://dx.doi.org/10.1016/j.compstruct.2017.05.059

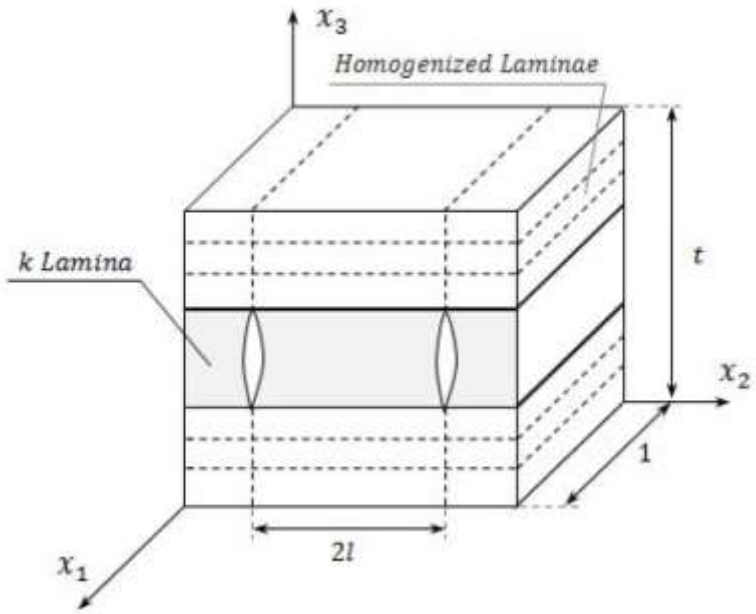

Fig. 1. Representative Volume Element (RVE).

Note that in (Eq.8) the stress $\sigma^{(k)}$ in each lamina is

$$\sigma^{(k)} = Q^{(k)} \cdot \left(\epsilon - \alpha^{(k)}\delta T\right) \quad \text{(Eq.9)}$$

where ϵ is the mechanical strain and $-\alpha^{(k)}\delta T$ is the thermal strain in lamina *k*. Thus, the elastic strain ϵ' in lamina *k* is

$$\epsilon' = \epsilon - \alpha^{(k)}\delta T \quad \text{(Eq.10)}$$

Next, mode decomposition is achieved by splitting the elastic strain energy release rate G between mode I (crack opening) and mode II (crack shear) as follows

$$U_I = \frac{V_{RVE}}{2H}\sum_{k=1}^{n} t_k\left(\epsilon_2 - {\alpha_2}^{(k)}\delta T\right) \cdot {Q_{2j}}^{(k)} \cdot \left(\epsilon_j - {\alpha_j}^{(k)}\delta T\right) \quad \text{(Eq.11)}$$

$$U_{II} = \frac{V_{RVE}}{2H}\sum_{k=1}^{n} t_k\left(\epsilon_6 - {\alpha_6}^{(k)}\delta T\right) \cdot {Q_{6j}}^{(k)} \cdot \left(\epsilon_j - {\alpha_j}^{(k)}\delta T\right) \quad \text{(Eq.12)}$$

where $\epsilon_6 = \gamma_{12}$, and using the coordinate system of the cracking lamina ($k = c$) so that the 2-component of strain produces crack opening mode I (crack opening) and the 6-component produces mode II (crack shear).

2.3. Damage activation function

In a purely thermal problem of a balanced laminate, including cross ply and quasi-isotropic laminates, the laminate expands or contracts without shear. Therefore $G_{II} = 0$ and G_{IIC} have no effect. However, applying mechanical loads on a laminate can cause a state of shear that may dominate the response.

Therefore, the following interaction criterion is used to predict damage initiation and evolution, as it has been thoroughly validated for not-thermal problems [6, 23].

$$g(\epsilon,\lambda) = (1-r)\sqrt{\frac{G_I(\epsilon',\lambda)}{G_{IC}}} + r\frac{G_I(\epsilon',\lambda)}{G_{Ic}} + \frac{G_{II}(\epsilon',\lambda)}{G_{IIc}} - 1 \leq 0 \qquad \text{(Eq.13)}$$

where $g \leq 0$ represents the undamaging domain and $r = G_{Ic}/G_{IIc}$. Note that no separate damage evolution equation and no additional material constants are needed. An increment of damage λ causes a reduction of stiffness, thus a reduction of G_I and G_{II}. Thus, the damage activation function shrinks inside the no-damage domain, Eq.(13). That means that an increment of strain ϵ' is needed to activate the damage again. This algorithm has been thoroughly validated for mechanical loads and it is further validated for thermo-mechanical loads in this work. The UGENS implementation uses two state variables (λ, g_{1t}) per ply, where λ is the crack density and g_{1t} is the highest value of longitudinal effective stress $g_{1t} = \sigma_1/(1-D_1)$, where D_1 is the damage of the fibers. D_1 can be calculated in terms of σ_1 so it is not necessary to store D_1 as a state variable. λ is a function of the elastic strain $\lambda(\epsilon')$. Both λ and g_{1t} are irreversible, so that do not decrease during unloading. The crack density is a function of the elastic strain ϵ' (Eq.10) and Cauchy stress σ through Eq.9.

3. PROBLEM DESCRIPTION

In this work, thermo-mechanically induced damage in open-hole composite laminates is studied. To solve this problem the new modifications made to DDM model are implemented in Abaqus using a UGENS user subroutine. The problem is solved using the finite element software ABAQUS/Standard. The problem definition includes the geometry of the plate, the elastic and strength properties of the material, and the stacking sequence of the laminate, as well as the temperature range for thermal induced damage and the mechanical load applied to the laminate for mechanical induced damage. The temperature range is specified with two predefined fields, one for the Stress Free Temperature (SFT) and another for the final temperature T_f. The mechanical load can be applied as either force or displacement on the boundary. Three different types of problem can be performed with DDM depending on the type of load applied to the laminate.

1. To study a pure **cooling thermal problem,** the Stress Free Temperature (SFT) and the end temperature (T_f) of the problem must be specified, where SFT is considered the initial temperature of the laminate. Both temperatures are introduced in the model as predefined fields applied to the whole

laminate. This problem set up for Abaqus with a "thermal" step represented as the difference between SFT and the end temperature T_f.

2. To study a pure **mechanical problem** the temperature range must be zero and an edge force or displacement is applied to represent a uniaxial tensile load in the *x*-direction. This problem is set up for Abaqus with a "Strain" step.
3. Finally, to study a **thermo-mechanical problem**, a combination of the last two problems is done. First the thermal step is applied and then the strain step.

In order to validate the DDM model, several materials with different stacking sequences and different types of loads are analyzed (Table 1). The validation is done in terms of crack density evolution as a function of temperature or applied load depending on the case analyzed.

Table.1. Materials and laminates used to validate DDM with thermal, mechanical, and thermo-mechanical loads: P75/934 [24, 25], P75/ERL1962 [25], AS4/3501-6 [26], and AS4/8552 [4].

Material	Laminate	Type of Validation
P75/934	$[0_2/90_2]_s$	Thermal problem
P75/934	$[0/45/90/-45]_s$	Thermal problem
P75/ERL1962	$[0_2/45_2/90_2/-45_2]_s$	Thermal problem
AS4/3501-6	$[0_4/45_4/90_4/-45_4]_s$	Thermal problem
AS4/3501-6	$[0_4/45_4/90_4/-45_4]_s$	Mechanical and Thermomechanical problem
AS4/8552	$[0_2/90_4]_s$	Mechanical and Thermomechanical problem

The mechanical properties at room temperature and the geometry of the specimens of the different material analyzed in this work were taken from the literature and are shown in Table 2 and Table 3 respectively [4, 24-26]. For the numerical model, only a portion of the specimen is represented, modelling the laminate as a square plate with dimensions *W*x*W*, where *W* is the width of the specimen (Table 3). Once the model is validated (as it is done in section 4), one of the materials in Table 2 is selected to study the effect of thermo-mechanical loads on notched and unnotched laminates. In fact AS4/3501-6 is selected because this material is validated for both thermal and mechanical loads. For the notched laminate, a hole of 2 mm radius is used.

Since unnotched laminates are subjected to a uniform state of strain, they are discretized with only 16 S4R elements (these are quadrilateral shell elements with 4 nodes and reduced integration). On the other hand, notched laminates that develop a non-uniform state of strain are discretized with 1188 S4R elements as shown in Fig. 2, with a mesh refinement close to the hole. In both cases, membrane only

boundary condition is considered and the full plate is modelled. Quarter symmetry cannot be applied because most of the laminates are quasi-isotropic. Since DDM model was demonstrated to be mesh independent in a previous work [6, 23], the purpose of using a fine mesh density is only to capture the stress and strain gradients.

Table 2. Mechanical properties at room temperature: P75/934 [24, 25, 37], P75/ERL1962 [24, 25, 38], AS4/3501-6 [26], and AS4/8552 [4].

Properties	Material			
	P75/934	**P75/ERL1962**	**AS4/3501-6**	**AS4/8552**
E_1 (GPa)	236	236	142.0	135
E_2 (GPa)	6.2	6.60	9.81	9.6
ν_{21}	0.29	0.29	0.30	0.3
G_{12} (GPa)	4.8	4.8	6.0	5.5
G_{Ic} (J/m^2)	40	104	141	1000
G_{IIC} (J/m^2)	60	648	458	2000
α_1 (με./ºC)	-1.22	-0.95	-0.36	0.28
α_2 (με./ºC)	28.8	39.60	28.8	28.0
SFT (ºC)	177	177	177	177
t_{ply} (mm)	0.127	0.127	0.134	0.134
Xt (MPa)	681.2	912.87	1950	2500
Xc(MPa)	306.82	441.26	1480	1531
Yc (MPa)	190.98	57.23	221	128

Table 3. Geometry of the specimens [4, 24, 25, 26].

Material and Laminate	**Length (mm)**	**Width (mm)**
P75/934 $[0_2/90_2]_S$	76.2	12.7
P75/934 $[0/45/90/-45]_S$	76	12
P75/ERL1962 $[0_2/45_2/90_2/-45_2]_S$	76	12
AS4/3501-6 $[0_4/45_4/90_4/-45_4]_S$	76.2	25.4
AS4/8552 $[0_2/90_4]_S$	230	10

Composite Structures, 183 (1) 510-520 (2018)
http://dx.doi.org/10.1016/j.compstruct.2017.05.059

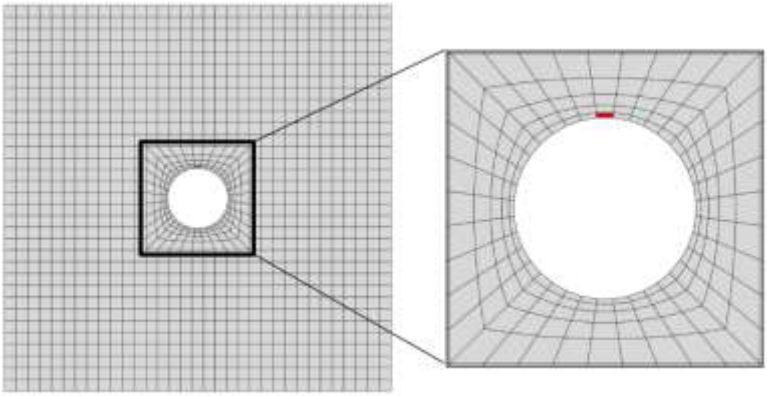

Fig. 2. Discretization of the plate. Notched laminate.

4. MODEL VALIDATION

DDM model validation is carried out for each of the types of load applied to the laminate: thermal load, mechanical load, and thermo-mechanical load.

4.1. Thermal-only loading

The evolution of crack density in laminates subjected to only thermal load (thermal problem) is predicted and compared with experimental data from [24-26]. Four materials and five different stacking sequences are studied, as shown in Table 1. The range of temperature variation is from SFT (assumed to be 177 º for most carbon fiber epoxy composites) to -184º C.

The matrix cracking growth in a thermal problem is represented by the crack density evolution respect to the temperature, as shown in Fig. 3 to 6. Good correlation between numerical results and experimental data is found. Especially accurate is the prediction of damage initiation.

For P75/934 $[0_2/90_2]_S$ laminate, good agreement between experimental and numerical results is found in Fig. 3. In this case the crack density evolution is the same in the 0º and 90º plies because when applying only thermal loads on a balanced cross-ply laminate, both plies behaves in the same way. In other words, there is no preferred orientation.

The differences between numerical and experimental results in 90º ply of P75/934 $[0/45/90/-45]_S$ laminate (Fig. 4.a) are higher than in the laminate $[0_2/90_2]_S$ of the same material (Fig. 3). The authors of these experimental tests stated that the evolution of crack density in this case are atypical and suggested that this behavior may be due to damage generated during the specimen preparation [25]. It is also important to note the scattering of the experimental results for this laminate. These facts could explain the higher differences observed between model and experiments. Nevertheless, the model matches both initiation and evolution in 45º ply (Fig. 4.b), considering the large scatter in the experimental data.

Composite Structures, 183 (1) 510-520 (2018)
http://dx.doi.org/10.1016/j.compstruct.2017.05.059

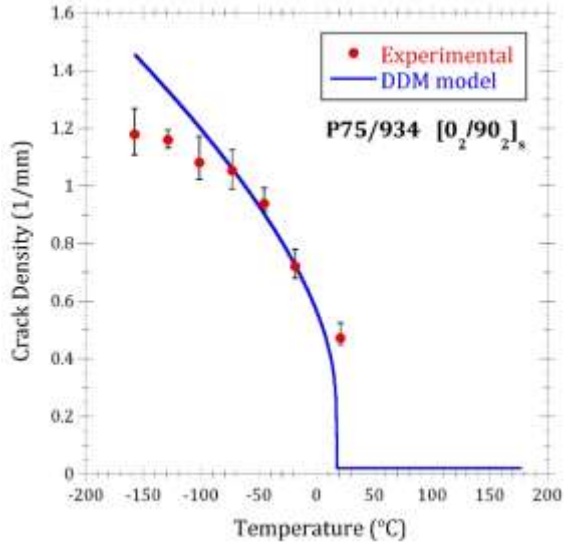

Fig. 3. Matrix cracking evolution with temperature in 0º and 90º plies. Laminate $[0_2/90_2]_S$. Material P75/934 [24]. Thermal-only problem.

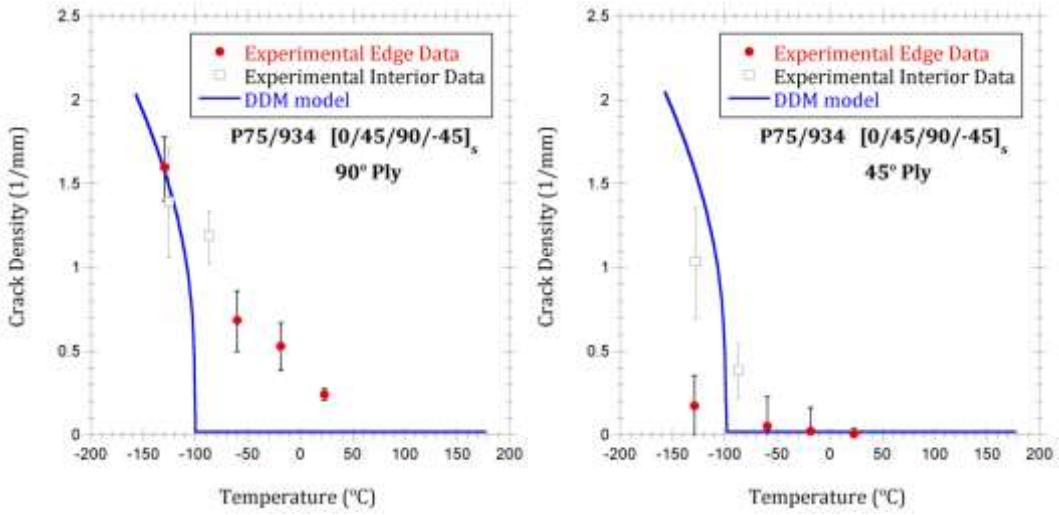

a) b)

Fig. 4. Matrix cracking evolution with temperature in laminate $[0/45/90/-45]_S$. Material P75/934 [25]. a) 90º ply, b) 45º ply. Thermal-only problem.

In Fig. 5, the differences observed for ±45º plies may be due to the complexity of observing and counting oblique cracks in ±45º plies experimentally. Some assumptions were made by the authors of those experimental tests in order to determine the presence or absence of a crack. For example, Park and McManus [25] counted as cracks only those that extend more than half the thickness of the ply; smaller crack (partial cracks) are not counted. Other authors [4] observed cracks with complex patterns (curved cracks or tree-type cracks); some of these cracks are counted as two or three straight cracks in order to draw the curve of crack density evolution. Those assumptions make it difficult to compare with numerical results because only crack which extend the whole thickness of the ply can be predicted by the model.

Also, in Fig. 5, experimental crack density was measured on older samples than the samples used to measure the mechanical properties including CTE [25]. Therefore, the numerical and experimental results may deviate from each other because the mechanical properties of the damaging specimens are not known with confidence.

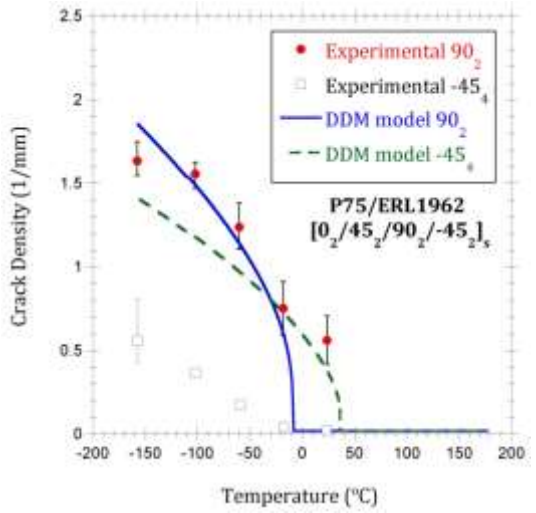

Fig. 5. Matrix cracking evolution with temperature in laminate $[0_2/45_2/90_2/\text{-}45_2]_S$, material P75/ERL1962 [25]. 90º ply and -45º ply. Thermal-only problem.

In Fig. 6, the predictions for AS4/3501-6 $[0_4/45_4/90_4/\text{-}45_4]_S$ are reasonably close considering the scatter of the experimental data. The differences observed between the numerical and experimental data in the 45º plies can be explained as before.

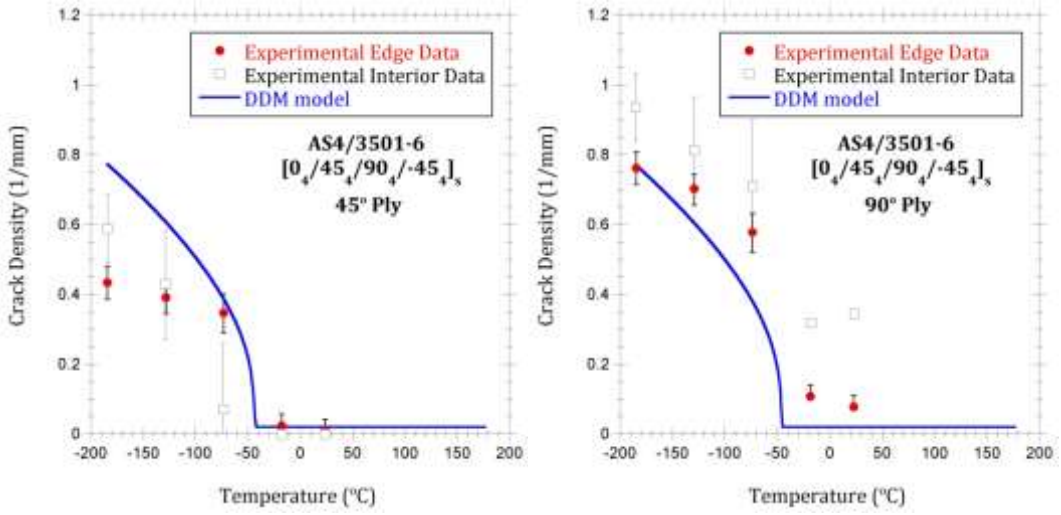

a) b)

Composite Structures, 183 (1) 510-520 (2018)
http://dx.doi.org/10.1016/j.compstruct.2017.05.059

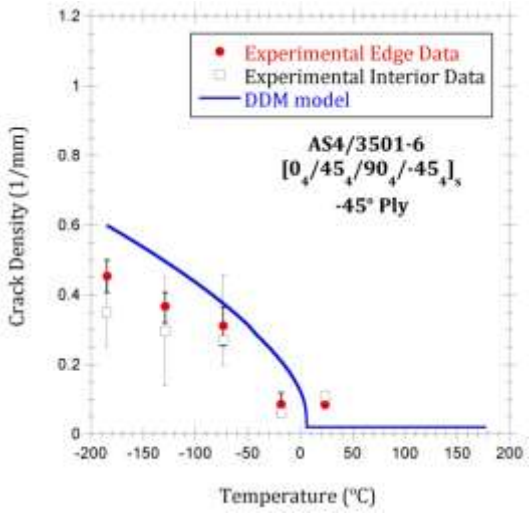

c)

Fig. 6. Matrix cracking evolution with temperature in laminate $[0_4/45_4/90_4/\text{-}45_4]_S$. Material AS4/351-06 [26]. a) 45º ply, b) 90º ply, and c) -45 ply. Thermal-only problem.

Considering all these facts, the results of the model can be considered reasonably accurate in thermal problems, without applying mechanical loads.

4.2. Mechanical and thermomechanical loading

In this section, the evolution of matrix cracking is predicted and compared for laminates subjected to either mechanical-only or combined thermomechanical load. Two cases are considered; one without thermal effect included in the model (mechanical problem) and another including the thermal stresses that appear in each ply (thermomechanical problem). In this validation, two materials and lay-ups are considered (Table 1).

Lundmark and Varna [4] studied the effect of thermomechanical loads at room temperature (RT) and at low temperature (LT). Only the results for RT are taken into account in the present work for the validation of the model because, for the same mechanical applied stress level, delaminations were found in the LT specimens, and delamination is not implemented in the current form of the DDM model.

The validation of the model when mechanical and thermomechanical loads are applied to the laminate is represented in Fig. 7 and 8 for AS4/3501-6 [26] and AS4/8552 [4], respectively. Cooling from SFT to 20ºC is applied first, followed by mechanical load. In Fig. 7, the thermal load slightly advances the onset of the damage with respect to mechanical load alone. Marginally higher damage was observed in the

thermo-mechanical problem compared with a mechanical-only problem for all ply-orientations. In 90º-plies, higher precision is obtained when the thermal load is included in the model (Fig. 7.b). The prediction of crack density evolution in ±45º plies is less accurate than in the other ply-orientations. The reason is the same as explained previously for thermal loads, namely the difficulty in seeing and counting oblique cracks, as noted in [25].

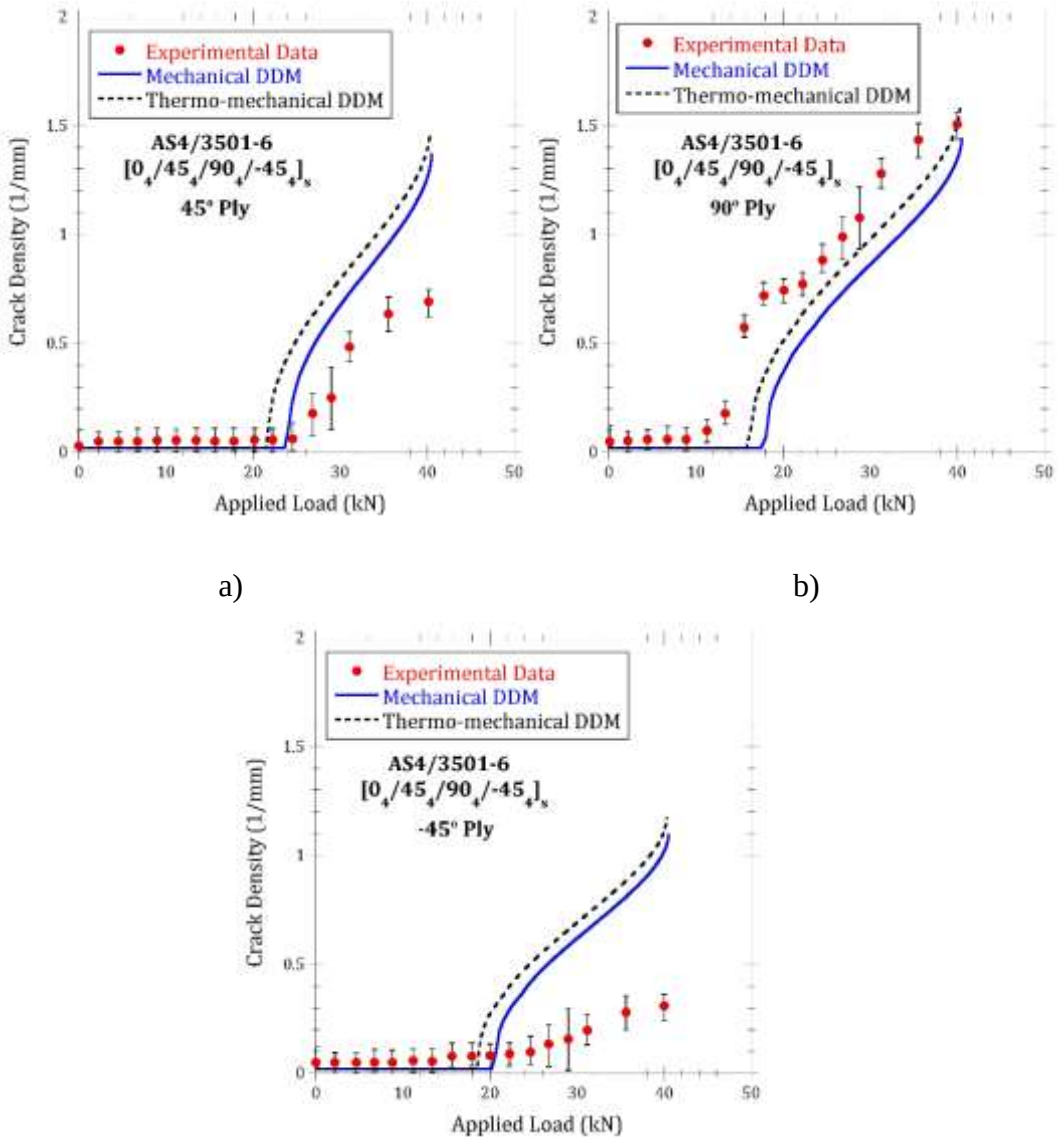

Fig. 7. Matrix cracking evolution in laminate $[0_4/45_4/90_4/-45_4]_s$. Experimental results for AS4/351-06 [26]. a) 45º ply, b) 90º ply, and c) -45 ply. Mechanical problem vs thermo-mechanical problem, cooled to room temperature of 20 ºC.

Composite Structures, 183 (1) 510-520 (2018)
http://dx.doi.org/10.1016/j.compstruct.2017.05.059

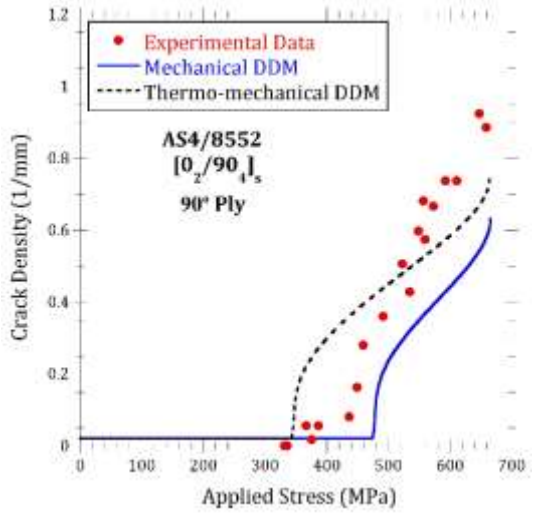

Fig. 8. Matrix cracking evolution in laminate $[0_2/90_4]_s$ for 90º ply. Experimental results for AS4/8552 [4]. Mechanical problem with $\Delta T = 0°C$ vs thermo-mechanical problem with $\Delta T = -157°C$.

In Fig. 8, a similar behaviour was observed for the AS4/8552 material. In this case, residual stress due to thermal load has a more noticeable effect than in Fig. 7.b, significantly advancing the initiation of damage with respect to the mechanical-only case. The model can predict the matrix cracking evolution in laminates subjected to both thermal and mechanical loads in laminates without holes.

5. NOTCHED LAMINATES

In this section, the behavior of quasi-isotropic open-hole laminates subjected to mechanical and thermomechanical loading is analyzed. From the results shown in the previous section, the material AS4/3501-6 and the stacking sequence $[0_4/45_4/90_4/-45_4]_s$ is selected because it has been validated both for thermal and mechanical loads. The influence of thermal and mechanical loads, separately and simultaneously, over notched and unnotched laminates is analyzed in this section.

For notched laminates, crack density is measured in the element located at the edge of the hole perpendicular to the load direction (red element in Fig. 2), because this point is where the highest stress appears. There are no differences in crack density for notched or unnotched laminates as long as they are subjected to the same thermal load (Fig. 9.a). The hole is not working as a stress concentrator when only thermal load is applied, and therefore the damage grows in all directions at the same time due to the quasi-isotropic behavior of this lay-up.

Once the thermal load has been applied (-184ºC in Fig. 9.a) a residual damage (crack density) associated to the applied thermal load remains on the laminate (starting values shown at 0 kN in Fig. 9.b). If subsequently a mechanical load is applied on both notched and unnotched laminates, the laminate containing the hole damages faster compared to the unnotched laminate due to the stress concentration associated to the hole (Fig. 9.b).

If only mechanical loads are applied to the laminate ($\Delta T = 0°C$ in Fig. 9.c) again the notched laminate damages more than the unnotched laminate, due to the stress concentration generated by the hole. However, crack density evolution in each ply are similar for both notched and unnotched laminates, even though the applied load is higher for unnotched laminates. The crack density is the same for notched and unnotched laminates because they have the same σ_2, thus same ϵ_2', thus same $\lambda(\epsilon_2')$.

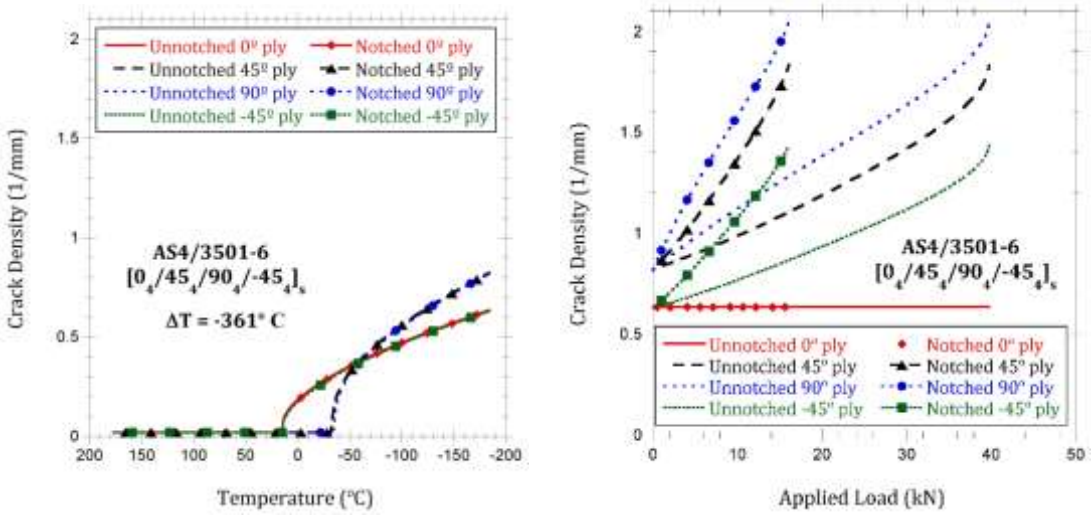

a) b)

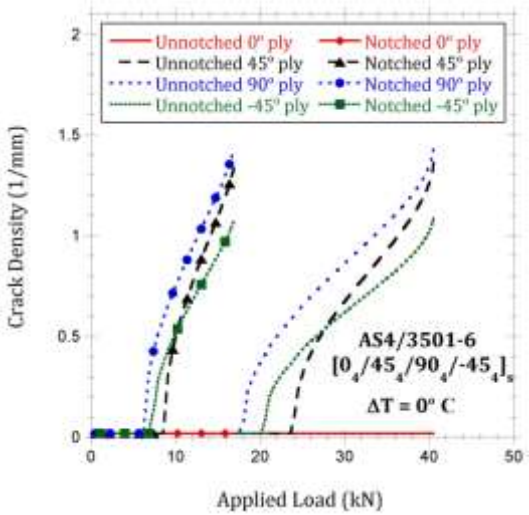

c)

Fig. 9. Matrix cracking evolution for AS4/3501-6 $[0_4/45_4/90_4/-45_4]_S$ laminate [26]. a) Thermal-only problem with $\Delta T = -361°C$ (mechanical load = zero), b) Mechanical problem for thermal load constant $\Delta T = -361°C$ carried from (a), and c) Mechanical-only problem with $\Delta T = 0°C$.

When a thermal cooling up to -184ºC is applied ($\Delta T = -361°C$), all plies of the laminate damage (Fig. 9.a). Plies oriented at 0º and -45º (surface and center ply) evolve in the same way and the same happen with 45º and 90º plies (interior plies). Under mechanical load, the crack density differs depending if the laminate has a hole or not. As expected, notched laminates damage faster than unnotched laminates (Fig. 9.b), and this is due to the stress concentration associated to the hole. However, the value of the maximum damage (maximum crack density) reached in both cases (notched and unnotched) is the same, while the applied load is smaller for the notched laminate. Also as per Fig. 9.b and 9.c, notched laminates damage faster than unnotched laminates, whether a thermal load is applied before the mechanical load (Fig. 9.b) or not (Fig. 9.c).

For unnotched laminates, the plots in Fig. 9.b and 9.c are terminated when the laminate reaches the peak load in the applied load vs. strain curve (points A in Fig. 10.a and D in Fig. 10.b); that is when the applied load reaches 39.873 kN and 40.521 kN for $\Delta T = -361°C$ and $\Delta T = 0°C$, respectively. It can be seen that the effect of thermal stresses on predicted peak load is small (1.60% difference). For notched laminates, plots in Fig. 9.b and 9.c are terminated when the tensile strength of the fiber is reached in the 0º laminas; that is when the applied load reaches 16.116kN and 16.926kN for $\Delta T = -361°C$ (point B in Fig. 10.a) and $\Delta T = 0°C$ (point D in Fig. 10.b), respectively. In this case also, the effect of thermal stresses on laminate failure load is small (4.79% difference). This happens even as the stress concentration factor (SCF) reaches $SCF = 2.47$ and $SCF = 2.40$ for $\Delta T = -361°C$and $\Delta T = 0°C$, respectively. Note that SCF increases only 2.92% when the thermal load is considered. These results suggest that residual thermal stress have no significant effect on SCF or ultimate load.

Despite residual thermal effect having no significant effect on SCF, the crack densities on 90º plies at failure are quite different, i.e., $\lambda = 2.05\ mm^{-1}$ and and $\lambda = 1.43\ mm^{-1}$ for $\Delta T = -361°C$ and $\Delta T = 0°C$, respectively (43.35% increase when thermal load is included). Similar behavior is observed for the rest of plies. Therefore, it would appear that crack density has no noticeable effect on SCF, at least for AS4/3501-6 quasi-isotropic. Furthermore, for each condition (thermal load applied or not) and just prior to laminate ultimate failure, the amount of matrix-damage in the critical element (at the edge of the hole) is the same as the distributed matrix-damage for the unnotched laminate. In fact the matrix-damage

Composite Structures, 183 (1) 510-520 (2018)
http://dx.doi.org/10.1016/j.compstruct.2017.05.059

are $\lambda = 2.05\ mm^{-1}$ and $\lambda = 1.43\ mm^{-1}$ with and without thermal load, respectively, at both the critical element of the notched laminate and everywhere for the unnotched laminate. In other words, for both, notched and unnotched laminates, matrix damage has to reach the same value ($\lambda = 2.05\ mm^{-1}$) for the laminates with thermal load ($\Delta T = -361°C$) to fail. Similarly, for both notched and unnotched laminates, matrix damage has to reach the same value ($\lambda = 1.43\ mm^{-1}$) for the laminates without thermal load ($\Delta T = 0°C$) to fail. This happens despite the fact that the notched laminate has failure load about 2.40--2.47 times lower than the unnotched laminate. When thermal load is applied, matrix-damage is larger (43% higher), but laminate failure is still controlled by stress concentration that mostly affects the longitudinal 0º laminas. In fact the model, which is capable of detecting fiber failure [6,23], indeed detects that the longitudinal tensile strength F_{1t} is reached in the longitudinal (0º) laminas just prior to laminate failure, and in all cases triggers the failure of the entire laminate. Thus, fiber failure is the final cause of failure.

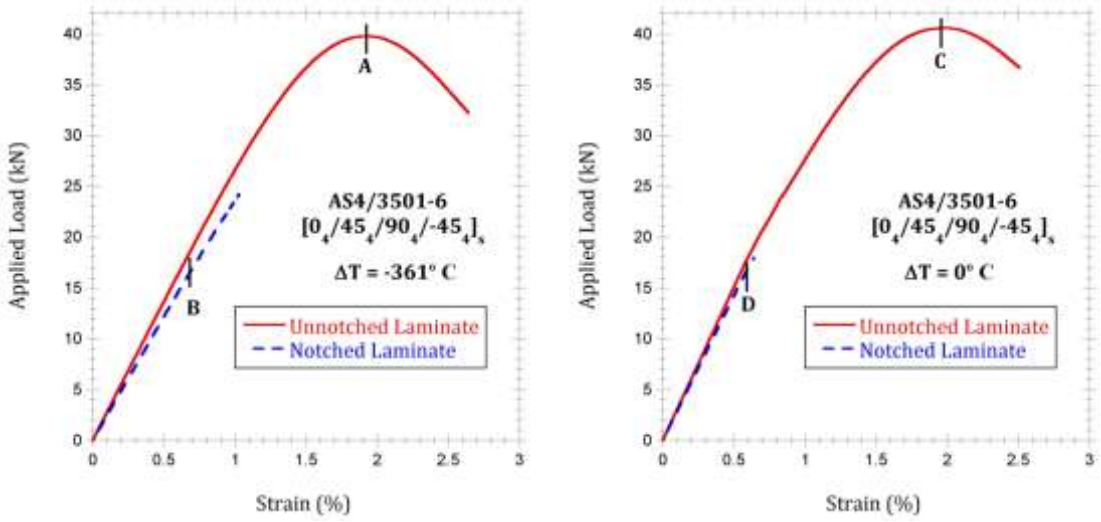

a) b)

Fig. 10. Applied load vs. strain curves for the mechanical load state in: a) Thermo-mechanical problem with $\Delta T = -361°C$ and b) Mechanical-only problem ($\Delta T = 0°C$)

In view of the results shown in Fig. 9, it can be concluded that by applying only thermal loads on notched or unnotched laminates, the notch does not affect the damage of the laminate. However, when a mechanical load is applied to a notched laminate, it damages faster than the same laminate without notch.

Composite Structures, 183 (1) 510-520 (2018)
http://dx.doi.org/10.1016/j.compstruct.2017.05.059

In Fig. 9, the thermal load was taken all the way to -184ºC before applying the mechanical load. In Fig. 11, Thermo-Mechanical induced damage on open-hole laminates is analyzed on the same laminate but stopping the thermal loads at 20ºC, 0ºC and -50ºC, respectively. Crack density is shown for the element situated above the hole (red element in Fig.1). Crack density for the thermal load (at 20ºC, 0ºC and -50ºC) is presented in Fig. 11.a,c,e, respectively. Crack density while applying mechanical load is shown in Fig. 11.b,d,f.

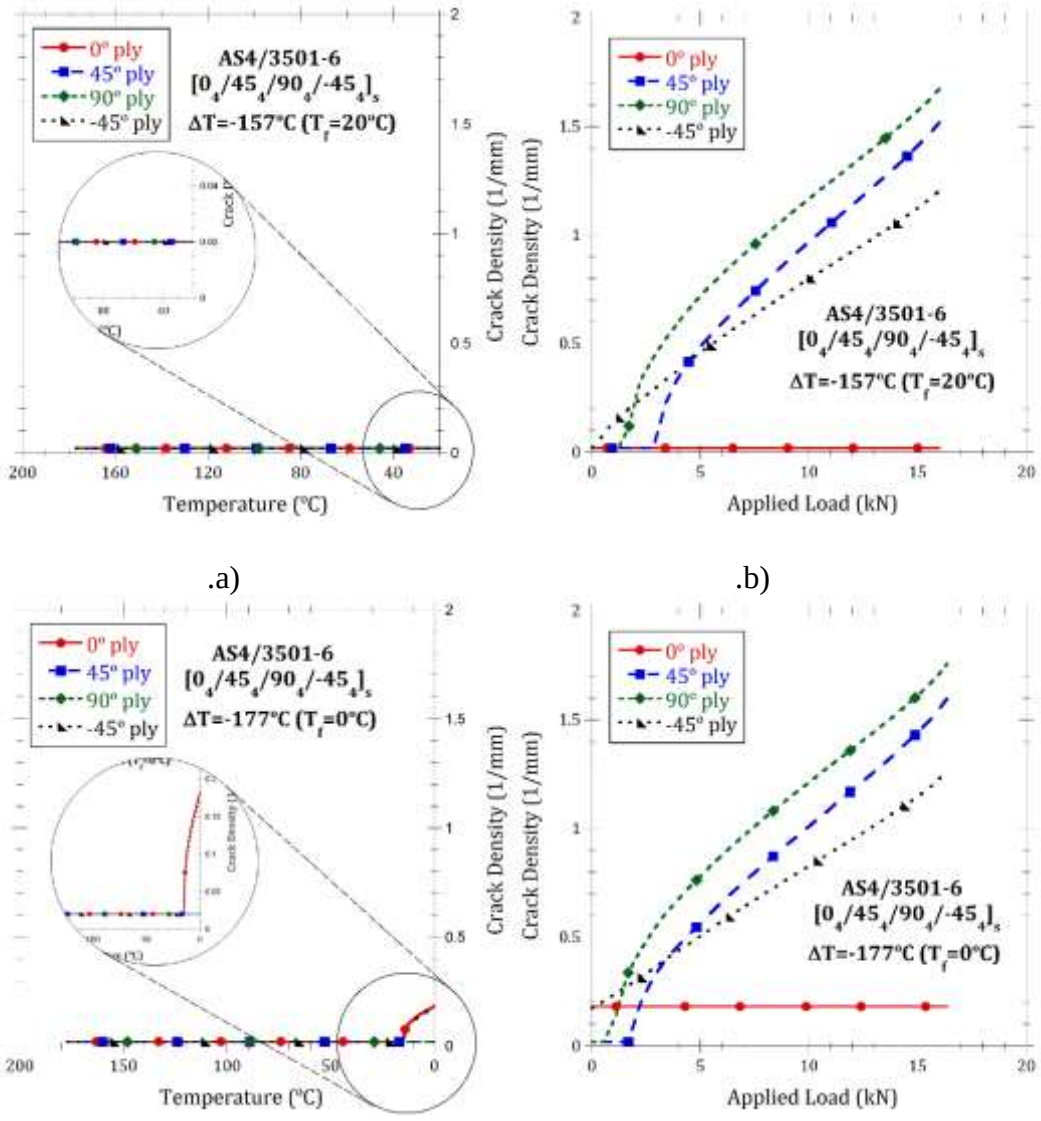

Composite Structures, 183 (1) 510-520 (2018)
http://dx.doi.org/10.1016/j.compstruct.2017.05.059

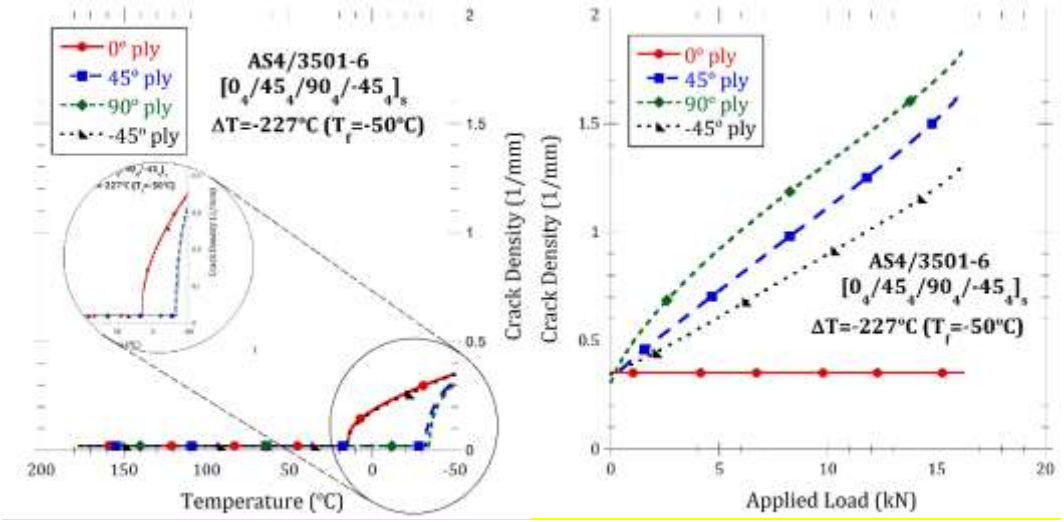

.e) .f)

Fig. 11. Matrix cracking evolution in each ply for notched AS4/3501-6 $[0_4/45_4/90_4/-45_4]_s$ for different thermal loads (Fig. 11.a,c,e) and subsequent mechanical load (Fig. 11.b,d,f).

When a thermal load equal to 20ºC is applied no thermal damage is observed in any of the plies. The small value observed in the zoom of Fig.11a is equal to the initial value introduced in the model to assure the convergence (0.02 mm-1). For lower temperatures (0ºC and -50ºC) a small increment of damage is observed (Fig. 11 c and 11e) before applying the mechanical load. Then, after that, while applying a mechanical load, the crack density continues with the value reached for the thermal load.

It can be seen that the thermal damage (nearly zero in Fig. 11.a and non-zero in Fig. 11.c and 11.e) remains constant for the 0º ply during subsequent mechanical load. Damage in 0º ply stops when the thermal load stops because mechanical load in *x*-direction does not increase crack density in 0º ply. However, fiber damage does occur in 0º ply due to mechanical load. For the other plies, mechanical load produces more damage. Damage in 0º and -45º plies start earlier because these are exterior and center plies respectively. Damage in interior plies 45º and 90º (thinner plies) start later but grow faster.

Crack density contour plots are discussed for T_f = -50ºC (Fig. 12 left) and T_f = -50ºC with full mechanical load (Fig. 12 right). Left images of Fig. 12 corresponds to the first step of the mechanical load applied to the laminate after applying a cooling temperature of T_f = -50ºC. Right images correspond to the final step after applying the full mechanical load. State variables SDV1 $= \lambda^0$, SDV11 $= \lambda^{45}$, SDV21 $= \lambda^{90}$ and SDV31 $= \lambda^{-45}$ are represented from the top to the bottom of the figure corresponding to the crack density on 0º, 45º, 90º and -45º plies of the laminate, respectively.

Composite Structures, 183 (1) 510-520 (2018)
http://dx.doi.org/10.1016/j.compstruct.2017.05.059

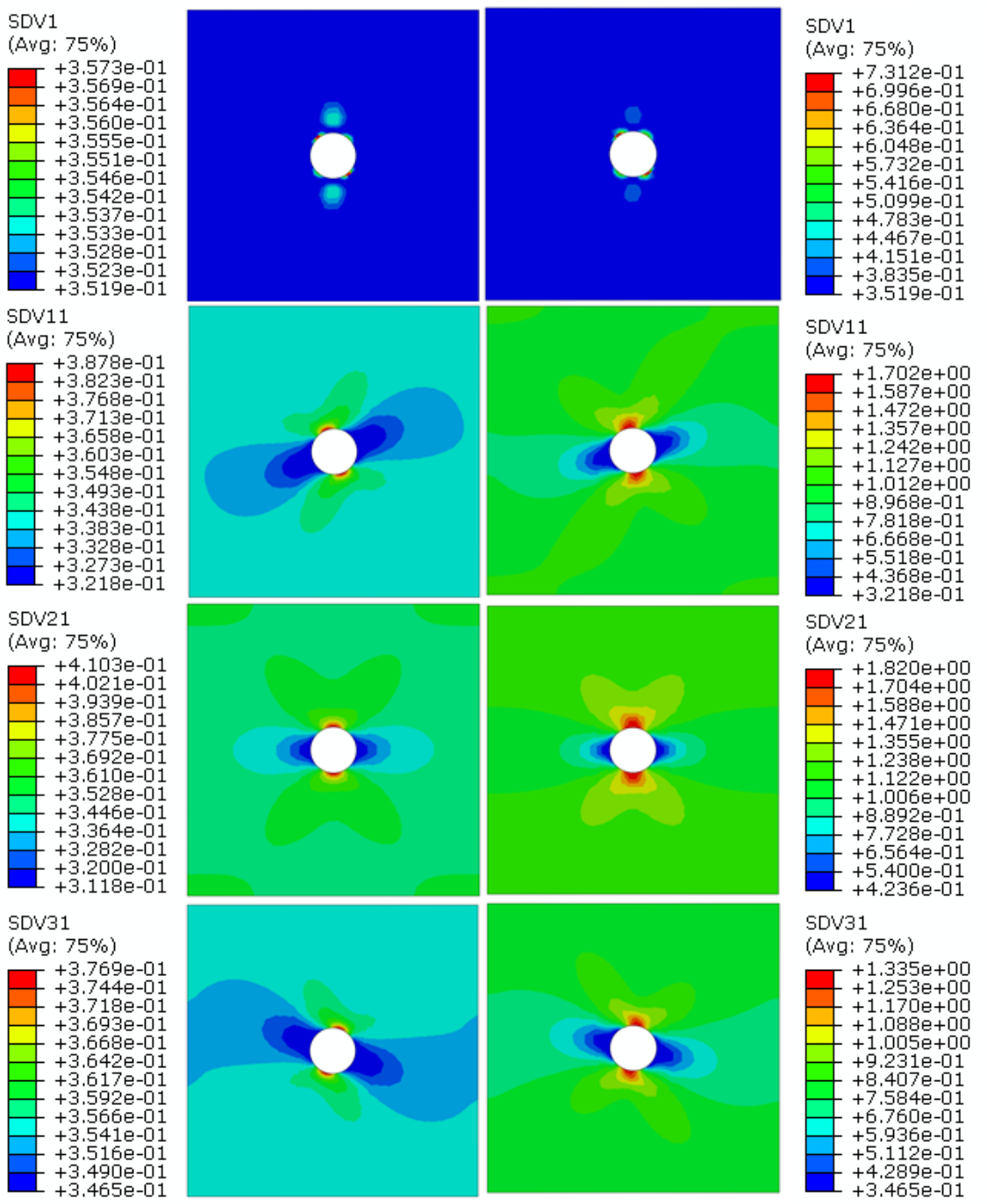

Fig. 12. Crack density contour plots for each ply of the laminate $[0_4/45_4/90_4/\text{-}45_4]_S$. State variables $\text{SDV1} = \lambda^0$, $\text{SDV11} = \lambda^{45}$, $\text{SDV21} = \lambda^{90}$ and $\text{SDV31} = \lambda^{-45}$ correspond to the crack density on 0º, 45º, 90º and -45º plies of the laminate, respectively. Left images corresponds to the first step of the mechanical load applied to the laminate after applying a cooling temperature of T_f = -50ºC. Right images correspond to the final step after applying the full mechanical load.

Composite Structures, 183 (1) 510-520 (2018)
http://dx.doi.org/10.1016/j.compstruct.2017.05.059

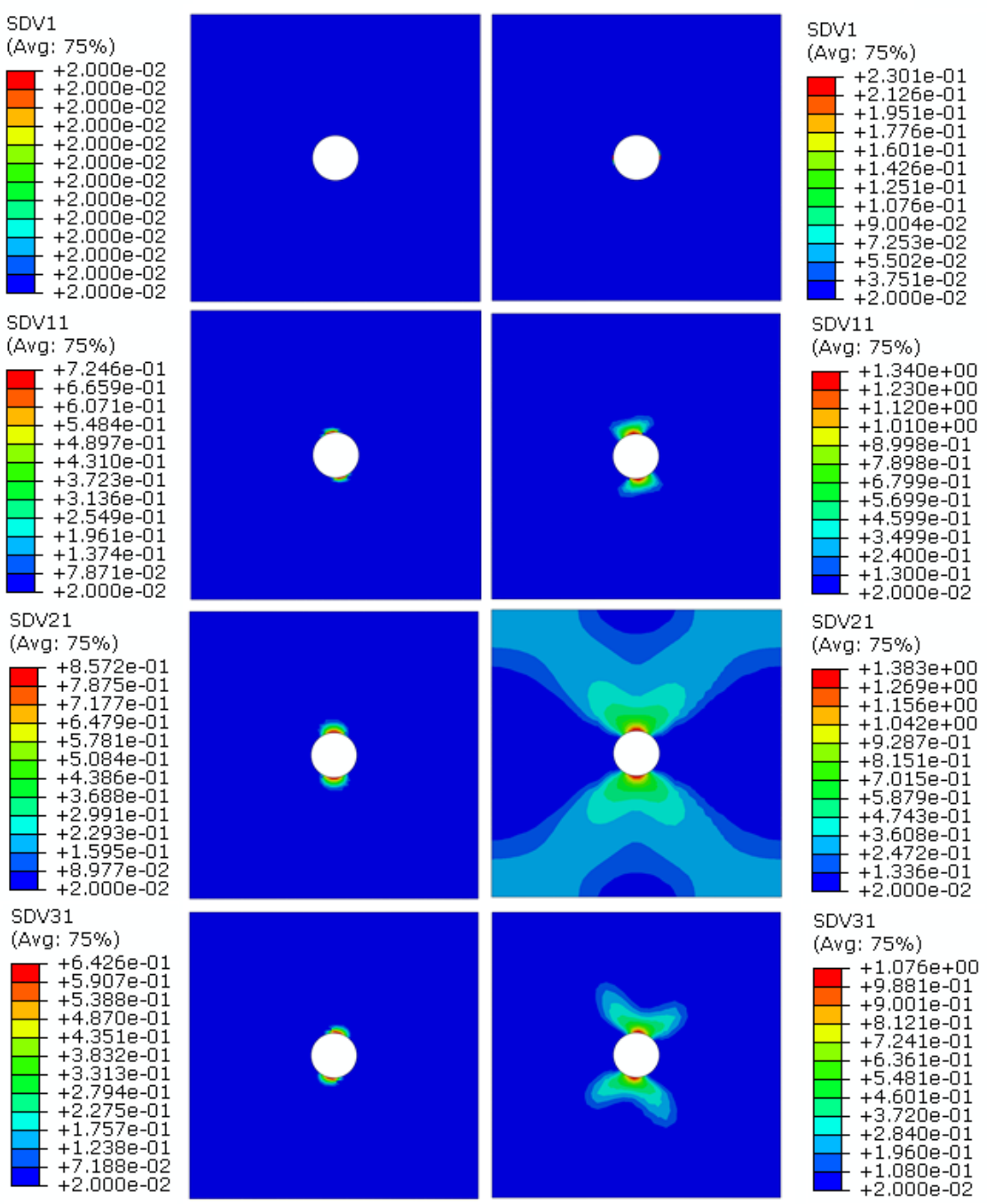

Fig. 13. Crack density contour plots for each ply of the laminate $[0_4/45_4/90_4/\text{-}45_4]_S$. State variables $\text{SDV1} = \lambda^0$, $\text{SDV11} = \lambda^{45}$, $\text{SDV21} = \lambda^{90}$ and $\text{SDV31} = \lambda^{-45}$ correspond to the crack density on 0º, 45º, 90º and -45º plies of the laminate, respectively. Left images corresponds to the first step of the mechanical load applied to the laminate. Right images correspond to the final step after applying the full mechanical load.

When a thermomechanical load is applied to the laminate, before applying the mechanical load, matrix cracking is uniform in all plies of the laminate, with magnitude $\lambda = 0.35, 0.32, 0.31$ and 0.35 $1/\text{mm}$ for 0º, 45º, 90º and -45º, respectively (not shown in Fig. 12). After that, when applying the mechanical load, for the first step (Fig. 12 left) the crack density is almost uniform for each ply, observing a slight concentration of damage close to the edge of the hole. After applying the full mechanical load, the crack density at the edge of the hole is much higher due to the stress concentration associated to the hole (Fig. 12 right). The damage in 0º ply is negligible compared to the rest of plies. It can be concluded that the typical concentration of damage near the hole only appears due to mechanical load. The effect of thermal load is to precipitate such damage earlier in terms of load and to make it larger in magnitude.

When only a mechanical load is applied to the laminate (Fig. 13), the value of the crack density before applying the load is 0.02 1/mm in each ply. For the first step of mechanical load (Fig. 13 left) a concentration of damage is observed around the hole, except for 0º ply which is not damaged. At full mechanical load (Fig. 13 right), 90º ply is the most damaged while 0º ply is not damaged at all. Also -45º ply damage earlier than 45º ply because it is a center ply, but at the end of loading the 45º accumulates more damage because it is a thinner inner ply.

6. CONCLUSIONS

In this work, matrix cracking and fiber damage evolution in laminates subjected to thermomechanical loads are analyzed by using a Discrete Damage Mechanic model. Experimental data for several material and lay-up are used to validate the model. Model predictions compare reasonably well with thermal-only, mechanical-only, and thermomechanical predictions if one allows for the scatter and uncertainty of material properties. For balanced symmetric laminates, including quasi-isotropic and cross-ply, the residual thermal stresses are not affected by the presence of a hole, because the laminate contracts uniformly, but mechanical loads are magnified by the SCF introduced by the notch. Thermal load may or may not initiate damage depending on δT and material properties, but always precipitates mechanically-induced damage, that is, it causes mechanically-induced damage to appear earlier and to accumulate at faster rate. It was found that ultimate load-carrying capacity of the laminate is reduced by the presence of a notch, and can be described by stress concentration factor. The mechanism of laminate failure is shown to be stress redistribution from the cracked laminas to the longitudinal laminas until the later reach their longitudinal tensile strength. This is shown to be the case for both notched and unnotched laminates with and without thermal loads.

Composite Structures, 183 (1) 510-520 (2018)
http://dx.doi.org/10.1016/j.compstruct.2017.05.059

ACKNOWLEDGEMENTS

The authors are indebted for the financial support of this work to the Ministry of Economy and Finance of Spain (project DPI2013-42240-R).

REFERENCES

[1] García-Castillo SK, Sánchez-Sáez S, Barbero E, Navarro C. Response of pre-loaded laminate composite plates subject to high velocity impact. J Phys IV 2006;134:1257-1263.

[2] Roy S, Utturkar A, Benjamin M. Modeling of permeation and damage in graphite/epoxy laminates at cryogenic temperatures. In: 45th AIAA/ASME/ASCE/AHS/ASC Structures, Structural Dynamics & Materials Conference. Palm Springs-California, April, 2004.

[3] Hodge AJ. Evaluating of microcraking in two carbon-fiber/epoxy-matrix composite cryogenic tanks. NASA/TM-2001-211194.

[4] Lundmark P, Varna J. Damage evolution and characterisation of crack types in CF/EP laminates loaded at low temperatures. Eng Fract Mech 2008;75:2631-2641.

[5] Lundmark P, Varna J. Constitutive relationships for laminates with ply cracks in-plane loading. Int J Damage Mech 2005;17:235-259.

[6] Moure MM, Otero F, Garcia-Castillo SK, Sanchez-Saez S, Barbero E, Barbero EJ. Damage evolution in open-hole laminated composite plates subjected to in-plane Compos Struct 2015;133:1048-1057.

[7] Park CHS. Analysis of thermally induced damage in composite space structures. Master Thesis at the Massachusetts Institute of Technology 1994.

[8] Timmerman JF, Tillman MS, Hayes S, Seferis JC. Matrix and fiber influences on the cryogenic microcracking of carbon fiber/epoxy composites. Compos Part A-Appl S 2002;33:323-329.

[9] Sánchez-Sáez S, Barbero E, Navarro C. Analysis of the dynamic flexural behaviour of composite beams at low temperature. Compos Sci Technol 2007;67:2616-2632.

[10] Ladeveze P. A damage Mechanics for composite materials. In: Dijksman JF, Nieuwstadt FTM, editors. Integration of theory and application in applied mechanics. Rolduc, Kerkrade, The Netherlands: Springer 1990 p 13-24.

[11] Talreja R. Damage characterization by internal variable, In: Pipes RB, Talreja R editors, Damage Mechanics of Composite Materials. Balkema, Rotterdam: Elsevier 1994 p 117-129.

[12] Barbero EJ, Cortes DH. A mechanistic model for transverse damage initiation, evolution, and stiffness reduction in laminated composites. Compos Part B Eng 2010;41:124-132.

[13] Maheo L, Dau F, André D, Charles JL, Iordanoff I. A promising way to model cracks in composite using Discrete Element Method. Compos Part B Eng 2015;71:193-202.

[14] Adumitroaie A, Barbero EJ. Intralaminar Damage Model for Laminates subjected to Membrane and Flexural Deformations. Mech Adv Mater Struc 2015;22:705-716.

[15] Gudmundson P, Ostlund S. First order analysis of stiffness reduction due to matrix cracking. J Compos Mater 1992;26:1009-1030.

[16] Gudmundson P, Ostlund S. Prediction of thermoelastic properties of composite laminates with matrix cracks. Compos Sci Techno 1992;44:95-105.

[17] Gudmundson P, Zang W. An analytic model for thermoelastic properties of compositelaminates containing transverse matrix cracks. Int J Solids Struct 1993; 30:3211-3231.

[18] Adolfsson E, Gudmundson P. Thermoelastic properties in combined bending and extension of thin composite laminates with transverse matrix cracks. Int J Solids Struct 1997;34:2035-2060.

[19] Adolfsson E, Gudmundson P. Matrix crack initiation and progression in composite laminates subjected to bending and extension. Int J Solids Struct 1999;36:3131-3169.

[20] Zang W, Gudmundson P. Damage evolution and thermoelastic properties of composite laminates. . Int J Damage Mech 1993;2:290-308.

[21] Adolfsson E, Gudmundson P. Matrix crack induced stiffness reductions in [(0m/90n/+p/-q)s]m composite laminates. . Compos Eng 1995;5:107-123.

[22] Lundmark P, Varna J. Modeling thermo-mechanical properties of damaged laminates. In: 3rd International Conference on Fracture and Damage Mechanics. Switzerland, Sept, 2003.

[23] Moure MM, Sanchez-Saez S, Barbero E, Barbero EJ. Analysis of damage localization in composite laminates using a discrete damage model. Compos Part B Eng 2014;66:224-232.

[24] Hugh L, McManus HL, Bowles DE, Tompkins SS. Prediction of thermal cycling induced matrix cracking. J Reinf Plast Compos 1996;15:124-140.

[25] Park CH, McManus HL. Thermally induced damage in composite laminates predictive methodology and experimental investigation. Compos Sci Techno 1996;56:1209-1219.

[26] Maddocks J. Microcracking in composite laminates under thermal and mechanical loading. Master Thesis at the Massachusetts Institute of Technology 1995

[27] Lee HJ, Saravanos DA. The Effect of Temperature Dependent Material Nonlinearities on the Response of Piezoelectric Composite Plates. NASA/TM-97-106216 1997

[28] Tompkins SS. Effects of thermal cycling on composite materials for space structures. NASA/SDIO Space Environmental Effects on Materials Workshop 1989:447-470.

[29] Gómez-del Río T, Zaera R, Barbero E, Navarro C. Damage in CFRPs due to low velocity impact at low temperature. Compos Part B Eng 2005;36:41-50.

[30] Kumagai S, Shindo Y, Horiguchi K, Takeda T. Mechanical characterization of CFRP woven laminates between room temperature and 4K. JSME Int J A-Solid M 2003; 46:359-364.

[31] Moure MM, García-Castillo SK, Sanchez-Saez S, Barbero E, Barbero EJ. Influence of ply cluster thickness and location on matrix cracking evolution in open-hole composite laminates. Compos Part B Eng 2016;95:40-47.

[32] Zhang J, Fan J, Soutis C. Analysis of multiple matrix cracking in [±θm/90n]s composite laminates, part {I}, inplane stiffness properties. Composites 1992; 23(5): 291-304

[33] Maligno AR, Warrior NA and Long AC. Finite element investigations on the microstructure of fibre-reinforced composites. Express Polymer Letters 2008; 2(9):665-676

[34] Sukjoo C and Sankar BV. Micromechanical Analysis of Composite Laminates at Cryogenic Temperature. Journal of Composite Materials 2006; 40(12):1-15

[35] Mingxian, W. Micromechanical Analysis of Thermally-Induced Deformations and Stresses in Unidirectional Continuous Carbon Fibre Reinforced Composites. Master thesis at the University of Manchester. 2011

[36] Barbero EJ. Introduction to Composite Materials Design. CRC PRESS, Philadelphia 2011.

[37] Derstine MS, Pindera MJ, Bowles DE. Combined mechanical loading of composite tubes. NASA-CR-183012, NAS 1.26:183012, CCMS-88-11, VPI-E-88-18. 1988

[38] Pisacane VL. Fundamentals of Space systems. Oxford University Press. 2005

[39] Barbero EJ, Cosso FA, Roman R, Weadon TL. Determination of material parameters for Abaqus progressive damage analysis of E-Glass epoxy laminates. Compos Part B Eng 2013;46:211-220.

Composite Structures, 183 (1) 510-520 (2018)
http://dx.doi.org/10.1016/j.compstruct.2017.05.059

FIGURE CAPTION

Fig. 1. Representative Volume Element (RVE).

Fig. 2. Discretization of the plate. Notched laminate.

Fig. 3. Matrix cracking evolution with temperature in 0º and 90º plies. Laminate $[0_2/90_2]_S$. Material P75/934 [24]. Thermal-only problem.

Fig. 4. Matrix cracking evolution with temperature in laminate $[0/45/90/-45]_S$. Material P75/934 [25]. a) 90º ply, b) 45º ply. Thermal-only problem.

Fig. 5. Matrix cracking evolution with temperature in laminate $[0_2/45_2/90_2/-45_2]_S$, material P75/ERL1962 [25]. 90º ply and -45º ply. Thermal-only problem.

Fig. 6. Matrix cracking evolution with temperature in laminate $[0_4/45_4/90_4/-45_4]_S$. Material AS4/351-06 [26]. a) 45º ply, b) 90º ply, and c) -45 ply. Thermal-only problem.

Fig. 7. Matrix cracking evolution in laminate $[0_4/45_4/90_4/-45_4]_s$. Experimental results for AS4/351-06 [26]. a) 45º ply, b) 90º ply, and c) -45 ply. Mechanical problem vs thermo-mechanical problem, cooled to room temperature of 20 ºC.

Fig. 8. Matrix cracking evolution in laminate $[0_2/90_4]_s$ for 90º ply. Experimental results for AS4/8552 [4]. Mechanical problem with $\Delta T = 0°\mathrm{C}$ vs thermo-mechanical problem with $\Delta T = -157°C$.

Fig. 9. Matrix cracking evolution for AS4/3501-6 $[0_4/45_4/90_4/-45_4]_S$ laminate [26]. a) Thermal-only problem with $\Delta T = -361°C$ (mechanical load = zero), b) Mechanical problem for thermal load constant $\Delta T = -361°C$ carried from (a), and c) Mechanical-only problem with $\Delta T = 0°C$.

Fig. 10. Applied load vs. strain curves for the mechanical load state in: a) Thermo-mechanical problem with $\Delta T = -361°C$ and b) Mechanical-only problem ($\Delta T = 0°C$).

Fig. 11. Matrix cracking evolution in each ply for notched AS4/3501-6 $[0_4/45_4/90_4/-45_4]_s$ for different thermal loads (Fig. 11.a,c,e) and subsequent mechanical load (Fig. 11.b,d,f).

Fig. 12. Crack density contour plots for each ply of the laminate $[0_4/45_4/90_4/-45_4]_S$. State variables $SDV1 = \lambda^0$, $SDV11 = \lambda^{45}$, $SDV21 = \lambda^{90}$ and $SDV31 = \lambda^{-45}$ correspond to the crack density on 0º, 45º, 90º and -45º plies of the laminate, respectively. Left images corresponds to the first step of the mechanical load applied to the laminate after applying a cooling temperature of T_f = -50ºC. Right images correspond to the final step after applying the full mechanical load.

Fig. 13. Crack density contour plots for each ply of the laminate $[0_4/45_4/90_4/-45_4]_S$. State variables $SDV1 = \lambda^0$, $SDV11 = \lambda^{45}$, $SDV21 = \lambda^{90}$ and $SDV31 = \lambda^{-45}$ correspond to the crack density on 0º, 45º,

90º and -45º plies of the laminate, respectively. Left images corresponds to the first step of the mechanical load applied to the laminate. Right images correspond to the final step after applying the full mechanical load.

TABLE CAPTION

Table.1. Materials and laminates used to validate DDM with thermal, mechanical, and thermo-mechanical loads: P75/934 [24, 25], P75/ERL1962 [25], AS4/3501-6 [26], and AS4/8552 [4].

Table 2. Mechanical properties at room temperature: P75/934 [24, 25, 37], P75/ERL1962 [24,25,38], AS4/3501-6 [26], and AS4/8552 [4].

Table 3. Geometry of the specimens [4, 24, 25, 26].